Theor Chem Acc (2003) 109:118–124
DOI 10.1007/s00214-002-0417-z

Theoretical
Chemistry Accounts

Regular article

A charge-scaling method to treat solvent in QM/MM simulations

Aaron R. Dinner[1], **Xabier Lopez**[2], **Martin Karplus**[3,4]

[1] Department of Chemistry, University of California, Berkeley, CA 94720, USA.
[2] Kimika Fakultatea, Euskal Herriko Unibertsitatea, P. K. 1072 20080 Donostia, Spain
[3] Department of Chemistry and Chemical Biology, Harvard University, 12 Oxford St., Cambridge, MA 02138, USA.
[4] Laboratoire de Chimie Biophysique, ISIS, Université Louis Pasteur, 4 Rue Blaise Pascal, 67000 Strasbourg, France

Received: 5 October 2001 / Accepted: 6 September 2002 / Published online: 28 February 2003

Abstract. We present a method to treat the solvent efficiently in hybrid quantum mechanical/molecular mechanical simulations of chemical reactions in enzymes. The method is an adaptation of an approach developed for molecular-mechanical free-energy simulations. The charges of each of the exposed ionizable groups are scaled, and the system is simulated in the presence of a limited number of explicit solvent molecules to obtain a reasonable set of structures. Continuum electrostatics methods are then used to correct the energies. Variations in the procedure are discussed with an emphasis on modifications from the original protocol. We illustrate the method by applying it to the study of a hydrolysis reaction in a highly charged system comprising a complex between the base excision repair enzyme uracil-DNA glycosylase and double-stranded DNA. The resulting adiabatic reaction profile is in good agreement with experiment, in contrast to that obtained without scaling the charges.

Keywords: Uracil – DNA glycosylase – Hybrid quantum mechanical/molecular mechanical simulation methods – Solvent shielding – Poisson – Boltzmann continuum electrostatics

1 Introduction

Hybrid quantum mechanical (QM)/molecular mechanical (MM) methods are widely used to model chemical reactions in enzymes [1, 2, 3, 4, 5, 6, 7]. In such simulations, the central reactive region is treated quantum mechanically to allow key bonds to be made and broken, while the surrounding non-reactive region is treated classically to make the calculations computationally feasible. Because one of the main goals of QM/MM studies is to understand how the environment influences the reaction of interest, adequate treatment of the solvent is essential. Solvent can play a direct role by interacting with the QM region, and it can play an indirect one by shielding MM groups and stabilizing selected MM conformations.

In simulations of enzymes, the solvent can be represented explicitly by including atomistic models of water molecules [8] or implicitly by adding terms to the energy function [9, 10, 11]. However, neither of these approaches is without problems. Explicit treatment of a sufficient number of water molecules to solvate an enzymatic system fully is costly because it is necessary to average over simulations that are much longer than the dipole relaxation time of water (about 10 ps at 300 K [12, 13]). Moreover, QM/MM simulations often employ only energy minimization, in which case, the effective dielectric will be much smaller than that associated with the true (thermalized) solvent reaction field. On the other hand, implicit treatment of the solvent in the vicinity of the reaction is also inappropriate if the lengths and directionalities of specific hydrogen bonds to water molecules play important roles [14].

In the present paper, we explore the use of a method that employs a combined explicit and implicit treatment of the solvent to avoid the shortcomings just described. The method is an adaptation to QM/MM calculations of an approach developed for free-energy perturbation simulations using molecular mechanics [15]. In brief, the charges of exposed groups are scaled to avoid distortion of the structures during the simulations, and continuum electrostatics methods are applied subsequently to obtain energies that introduce the correct solvent shielding effects. We illustrate the procedure by applying it to the study of a chemical reaction in a highly charged system consisting of a complex between an enzyme and double-stranded DNA. The QM/MM study models the hydro-

Contribution to the Proceedings of the Symposium on Combined QM/MM Methods at the 222nd National Meeting of the American Chemical Society, 2001

Correspondence to: M. Karplus
e-mail: marci@tammy.harvard.edu

lysis of the glycosyl bond of deoxyuridine (dU) in DNA by the base excision repair enzyme uracil-DNA glycosylase (UDG). The resulting adiabatic reaction profile is in good agreement with experiment [16], in contrast to that obtained without scaling the charges. Variations in the procedure are discussed with an emphasis on modifications from the protocol employed in the original free-energy-perturbation simulations [15].

2 Charge-scaling procedure

In this section, we describe the charge-scaling method that we use to treat solvent shielding in QM/MM simulations. Essentially, the charges of each of the exposed ionizable groups are scaled, and the system is simulated in the presence of a limited number of explicit solvent molecules to obtain a reasonable set of structures. Grid-based continuum electrostatics methods that employ the Poisson or linearized Poisson–Boltzmann equation are then used to estimate the energy required to return the scaled groups to their normal charge states and to transfer the structures to bulk solvent (Fig. 1). Details of this procedure are given in what follows with emphasis on aspects that differ from the original formulation for MM free-energy simulations [15].

In step I, the charges on exposed ionizable groups are scaled, and a simulation with a limited number of explicit solvent molecules is then performed. It was shown for MM calculations that the corrected energies obtained with this procedure do not depend on the specific scale factors employed, so long as the structural distortions associated with simulations in vacuum are reduced sufficiently [15]. This is not strictly true in QM/MM simulations owing to polarization of the QM region, so care must be exercised in choosing the scale factors. In the present study, we use the potential-based scheme suggested in Ref. [15]. Specifically, for a representative conformation of the system, which includes the explicit solvent molecules that are present in the simulation, we calculate the electrostatic potential, Φ, from each exposed ionizable group i by solving the Poisson equation in vacuum ($\epsilon = 1$) and in solution ($\epsilon = 80$). The scale factor for group i, α_i, is then the ratio of the average vacuum, $\bar{\Phi}_v$, and solution, $\bar{\Phi}_s$, potentials for the grid points occupied by the QM atoms (determined from their positions and van der Waals radii):

$$q_i' = \frac{\bar{\Phi}_s(i \rightarrow \mathrm{QM})}{\bar{\Phi}_v(i \rightarrow \mathrm{QM})} q_i = \frac{q_i}{\alpha_i}. \quad (1)$$

Alternative averaging schemes (e.g., averaging the ratios at points) did not change the scale factors appreciably since the potentials were relatively homogeneous over the QM region. In principle, salt effects could be included by solving the linearized Poisson–Boltzmann equation rather than the Poisson equation; however, the distributions of scale factors obtained with the two methods were similar, so all the results shown are for pure water. It is important to note that the α_i values

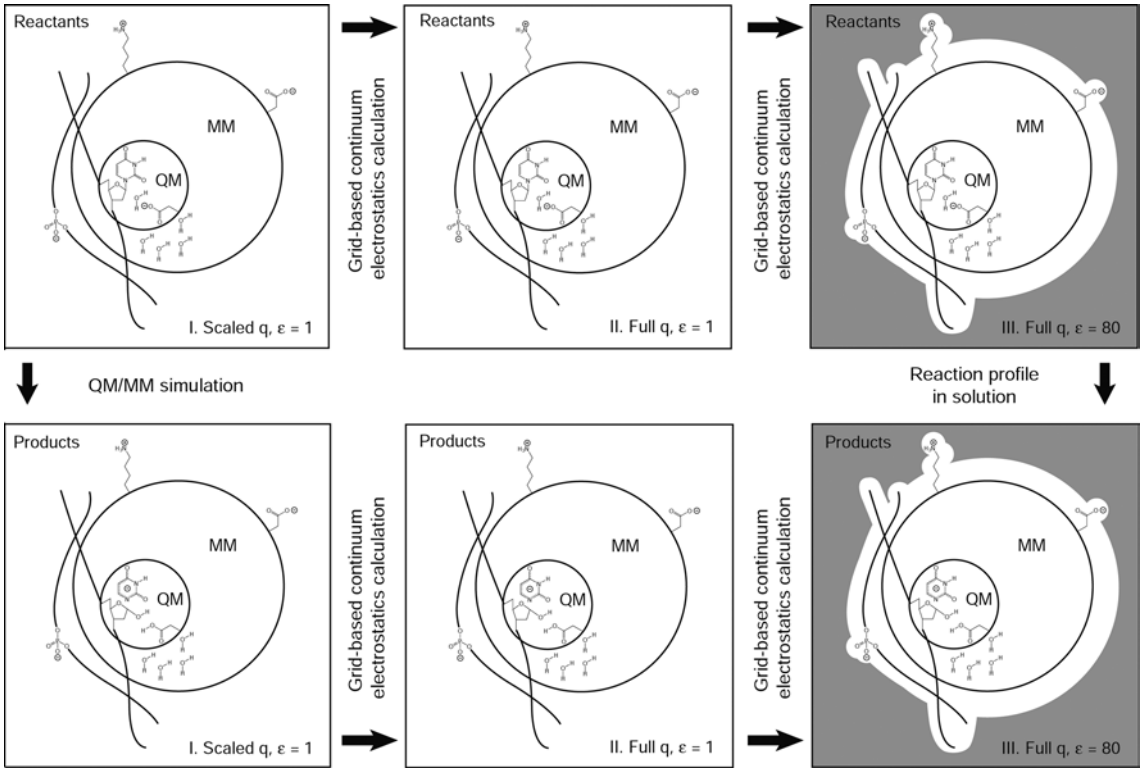

Fig. 1. Thermodynamic cycle employed in the charge-scaling procedure. Representative groups are illustrated by chemical structures: the quantum mechanical (QM) region, three ionizable groups (an aspartate side chain, a lysine side chain, and a phosphate group), and four explicit molecular mechanical (MM) water molecules

depend on the structure of the system but not the charge distribution in the QM region. As a result, it is reasonable to use constant scale factors to model a chemical reaction if the positions of the ionizable groups and the volume excluded by the explicit atoms do not deviate significantly from those of the representative structure used for the determination of the α_i values. If a large conformational change were involved in the process under study, the method would have to be modified. This issue was examined recently in a study of annexin V which employed a potential-based scheme to scale the charges but did not subsequently correct the energies [17]. There, scale factors were calculated separately for the endpoints of a reaction which involved the exposure of a tryptophan side chain and the complete unwinding of a helix. In that case, it was found that the two sets of α_i differed by only 3% on average, and constant (average) scale factors were thus used.

In step II of the procedure, we calculate the energy associated with restoring the scaled charges to their full values in vacuum for each structure saved from the simulation in step 1. In these and subsequent continuum electrostatics calculations, the QM atoms are represented by their Mulliken charges unless otherwise specified. For a given structure, the change in the effective energy of interaction between the exposed ionizable groups and the QM atoms is

$$\Delta W_{\mathrm{QM/MM}}(\{\alpha_i\} \rightarrow 1) = \sum_i \sum_j (1-\alpha_i) q_j \Phi_{\mathrm{v}}(i \rightarrow j), \quad (2)$$

where the first sum runs over the groups with scaled charges and the second sum runs over the grid sites on which the QM charges are distributed. Simonson et al. [15] neglected interactions between the scaled and MM groups (including other scaled groups) in this step and the subsequent (bulk solvation) (step III). Neglecting the scaled-MM terms is justified only if they do not affect the reaction profile significantly. In the example considered here, we found that this was not the case. Consequently, we include these terms; however, doing so introduces additional complications into the procedure for the following reasons. Because the grid-based calculations ignore the molecular connectivity of the system, they include classical electrostatic interactions between bonded atoms. These terms have no physical basis – interactions between bonded atoms should either be treated quantum mechanically or by a reasonable classical approximation such as a harmonic or Morse potential. When the charges of the scaled groups are increased to their full strengths, these unphysical (1–2 and 1–3) terms change by large amounts, so it is necessary to take precautions to eliminate or to avoid them. Two methods which differed in their computational cost were used to determine the energies for step II of the charge-scaling procedure. In the first (quicker) (IIa), $\Delta W_{\mathrm{QM/MM}}(\{\alpha_i\} \rightarrow 1)$ was calculated as previously, and the scaled-MM interaction terms were obtained from the CHARMM Coulomb electrostatic energy term (which omits 1–2 and 1–3 interactions [18]) with the charges on the QM atoms set to zero (to avoid double-counting the terms involving QM atoms). In the second method (IIb), only grid-based methods were used:

$$\Delta W(\{\alpha_i\} \rightarrow 1) = \sum_j q_j \Phi_{\mathrm{v}}(j) - \sum_j q'_j \Phi'_{\mathrm{v}}(j) - \sum_i \left[\sum_{j_i} q_{j_i} \Phi_{\mathrm{v}}(j_i) - \sum_{j_i} q'_{j_i} \Phi'_{\mathrm{v}}(j_i) \right], \quad (3)$$

where primes denote scaled charges, the sum over i runs over all scaled groups (e.g., the side chains of ionizable residues), the sum over j runs over all grid sites, and the sum over j_i runs over all grid sites containing charges associated with atoms in or bonded to scaled group i. In other words, $\sum_j q_j \Phi_{\mathrm{v}}(j)$ is the total energy, while $\sum_{j_i} q_{j_i} \Phi_{\mathrm{v}}(j_i)$ is the internal energy of scaled group i. The latter is necessary to remove the 1–2 and 1–3 interactions that change in step II (those that do not change cancel in the thermodynamic cycle). As for the interactions between the scaled groups and the QM atoms, Eq. (2) is subsumed within Eq. (3). Method 2b maintains better consistency with step III, which is based entirely on grid-based calculations, but omits 1–4 and sequentially longer-ranged electrostatic interactions within scaled groups (included in IIa).

In step III of the procedure, the system is transferred from vacuum ($\epsilon = 1$) to bulk solvent ($\epsilon = 80$). As in step II, a grid-based method is used to obtain the electrostatic free energy by solving the Poisson (or linearized Poisson–Boltzmann) equation. In both steps II and III, the QM atoms are represented by their Mulliken charges calculated in the presence of the MM atoms. The analysis of a subset of structures (see later) shows that electrostatic screening potential (ESP) charges [19, 20] give very similar results. The final corrected effective energies are the sums of the energies and electrostatic free energies obtained in steps I, II and III. The procedure differs from that in Ref. [15] in that Mulliken or ESP charges are used to represent the QM atoms (Ref. [15] concerns purely MM simulations) and scaled-MM interaction terms are included in steps II and III.

3 Simulation details

The system for which the present method was introduced is the base excision repair enzyme human uracyl DNA-glycosylase (UDG), which catalyzes the hydrolysis of the glycosyl bond of deoxyuridine (dU) in DNA. The reaction mechanism (Fig. 2) and its biological implications are described elsewhere [16]. A reactant structure was obtained by modeling the natural substrate in the active site on the basis of an enzyme- inhibitor complex (a preliminary version of PDB code 1EMH [21]) as detailed in Ref. [16]. The system employed in the calculations consists of the entire recombinant protein (223 residues, indexed according to their positions in the ***UNG*** gene: 82–304) [22], the bound double-stranded DNA oligomer, and 168 crystallographic water molecules (of which 22, including the catalytic one treated quantum mechanically, are within 6 Å of the QM atoms). One nucleic acid strand has nine nucleotides (indexed 2–10 with dU at 5), while the complementary strand has ten (indexed 21–30).

Standard protonation states were employed for all residues other than the histidines. On the basis of NMR data [23], H268 was taken to be neutral with the proton on N^{ϵ}. Continuum electrostatics methods [24] were used to determine the most probable protonation states of the 12 remaining histidines at neutral pH; the calculations indicated that H148, which forms a bridge between the

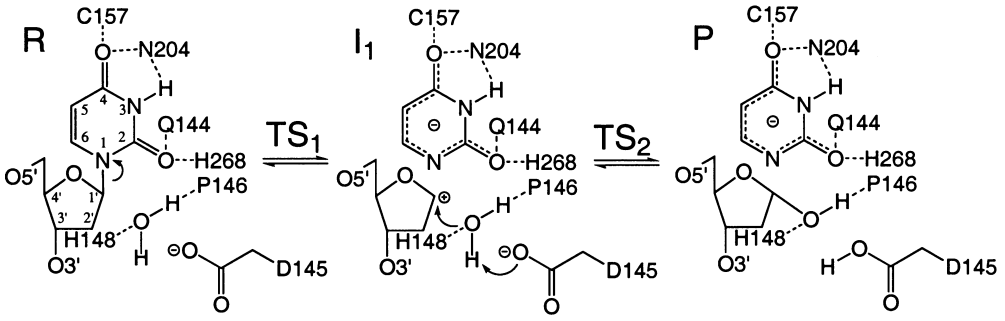

Fig. 2. Schematic of the reaction mechanism used to illustrate the charge-scaling procedure (see text)

phosphate group of dT4 and the attacking water molecule, is doubly protonated, while the other histidines are neutral with the proton on N^{ϵ}.

The reaction was modeled in the active site with a hybrid QM/MM method [1]. The uracil nitrogenous base, part of the sugar ring (C1′, C2′, C4′, O4′, and their associated hydrogen atoms), the attacking water, and the side chain of D145 were treated with the semiempirical method AM1 [25]. The remainder of the system, which included 167 additional crystallographic water molecules, was treated classically with the CHARMM all-hydrogen parameter set (that released with version c22 for the protein and that released with version c27 for the nucleic acid) [18, 26, 27] and the TIP3P water model [8, 28]. The MM nonbonded interactions were (force) shifted to zero over the range 8–12 Å [29], and the QM/MM interactions were truncated at 13 Å. The dielectric constant for the MM electrostatic interactions was $\epsilon = 1$, which is consistent with the QM calculation.

Because the boundary between the QM and MM regions crosses covalent bonds, it is necessary to terminate the QM region artificially. On the basis of a systematic comparison of methods for this purpose in Ref. [30], we introduced ("HQ") link atoms that interact with both the other QM atoms and the MM atoms. There are four such atoms, which correspond to the D145 C^{α}–C^{β} bond, the dU5 C2′–C3′ bond, the dU5 C3′–C4′ bond, and the dU5 C4′–C5′ bond. Linear geometries and crystallographic lengths were enforced for these bonds by adding harmonic restraints to the energy function. The charges on the MM atoms in these bonds were sufficiently small that it was not necessary to exclude QM/MM interactions with those atoms; setting the charges on those MM atoms to zero changed the energies by less than 1 kcal/mol.

The charge-scaling procedure was applied to the side chains of all eight arginines, the side chains of all 18 lysines, the side chains of all 12 glutamates, the side chains of the eight aspartates other than the catalytic one (D145), and all 17 phosphate groups. The scale factors were calculated by applying the potential-based scheme described in Ref. [15] to the X-ray crystal structure. To obtain an adiabatic energy surface, the system with the scaled charges was minimized in the presence of harmonic restraints on the breaking and forming bonds (Fig. 2). The continuum electrostatics calculations were performed with the Poisson–Boltzmann solver (PBEQ) in CHARMM versions c28a2 and c28a3. To determine the sites from which solvent was excluded, the van der Waals radii associated with the parameter set described previously were used in conjunction with a 1.4-Å-radius probe. The grid spacing was 1 Å in step 2 and 0.5 Å in step 3.

4 Results

The enzyme UDG shifts the reaction pathway from a concerted-associative solution mechanism with a barrier of 32.1 kcal/mol to a stepwise-dissociative mechanism with a barrier of 12.1 kcal/mol (Fig. 2) [16]. In the latter, the glycosyl bond breaks first to yield an oxocarbenium cation/anion intermediate; a water molecule then attacks at C1′ and in the process loses a proton to the general base D145. This is the first enzyme reaction for which the existence of a transiently stable oxocarbenium cation intermediate has been demonstrated experimentally [31] and theoretically [16]. Other enzymatic mechanisms that were proposed to involve such an intermediate (e.g., that of lysozyme) have been challenged recently [32], though the new evidence is not unequivocal. A representative set of structures along this reaction pathway were taken from the adiabatic energy surface obtained in Ref. [16] and are used here to show the contributions made by the different steps of the charge-scaling procedure to the total reaction profile.

As detailed in Sect. 3, we scaled the charges on 63 ionizable groups (the side chains of arginine, lysine, aspartate, and glutamate residues and the phosphate groups in the DNA backbone). A histogram of the scale factors obtained with the potential-based scheme [15] is shown in Fig. 3. The scale factors range from 1.6 to 74.8. In principle, scale factors larger than the solution dielectric ($\epsilon = 80$) can be obtained [33], but none is observed. Buried groups have lower scale factors than exposed ones; the figure suggests that most groups are at least partially buried. The three lowest scale factors are for phosphate groups that are buried upon substrate binding (dU5, dA6, and dT7 in ref. [16]).

The reaction profile and its decomposition into the various steps (1, 2, and 3) are shown in Fig. 4. The rate-limiting transition state (TS_1), which corresponds to the cleavage of the glycosyl bond, has an energy of 14.3 kcal/mol (all energies are relative to the reactants). The oxocarbenium cation/anion intermediate (I_1) has an energy of 5.8 kcal/mol and the subsequent transition state (TS_2), which corresponds to attack of a water molecule, has an energy of 9.7 kcal/mol. The final

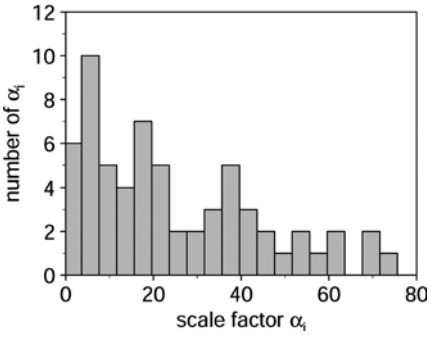

Fig. 3. Histogram of the scale factors for uracil-DNA glycosylase

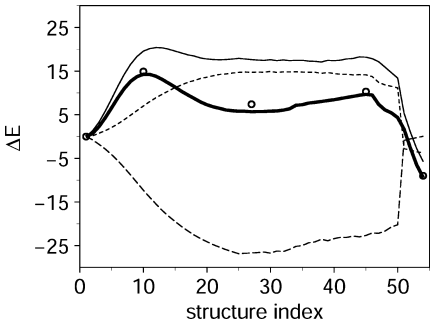

Fig. 4. Reaction profile obtained with Mulliken charges representing the QM atoms. Total (*bold solid line*), step I (*thin solid line*), step IIa (*long dashed line*), and step III (*short dashed line*) energies. The total energies obtained for the extrema by using method IIb instead of IIa (Sect. II) are indicated by *circles*

products have an energy of −9.4 kcal/mol. On examining the decomposition, we see that the overall shape of the reaction profile is determined by the initial simulation in the presence of the scaled charges (step I) but that the relative energies are modulated by the subsequent continuum electrostatics calculations (steps II and III). In particular, both TS_1 and I_1 are markedly higher in energy in step I. These states are stabilized by step II in which the charges of the ionizable groups are increased to their full strengths in vacuum. It was shown in Ref. [16] that the MM groups primarily responsible for this effect are the four phosphate groups that are buried upon substrate binding. Even though those groups have small scale factors (an average of 2.3), they make a large contribution owing to their proximity to the reaction. The effect of step III is in a direction opposite to that of step II, as expected. In essence, favorable electrostatic interactions are reduced by the addition of the dielectric which represents the solvent.

In contrast to the results just described, the reaction profile obtained in the absence of the charge-scaling procedure (not shown) is in complete disagreement with experiment. It resembles a sum of steps I and II. The initial barrier is reduced to 4.2 kcal/mol, and I_1 becomes the global energy minimum with $E = -11.7$ kcal/mol. The products do not correspond to a minimum on the energy surface because the proton transfer from the attacking water to the aspartate is drastically disfavored. Similar results are obtained even if additional water molecules are added to the system because the explicit solvent cannot reorganize significantly during energy minimization.

For the curves in Fig. 4, we used method IIa (Sec. 2) to determine the energy associated with increasing the charges on the ionizable groups to their full strengths. For comparison, the total energies obtained with method IIb are shown for the extrema (points in Fig. 4). For most structures, the energies obtained with the two methods for step II are within 1 kcal/mol; for I_1, the difference is 1.6 kcal/mol. Some of the differences are likely to stem from the fact that in method IIa, an average structure was used to calculate the potentials associated with the ionizable groups [$\Phi_v(i \rightarrow j)$ in Eq. 2], while in IIb the specific structures indicated were used. Even with this approximation, the "error" associated with using method IIa is comparable to the variation in energy expected from starting with a somewhat different initial structure. This suggests that use of the faster method (IIa) is a satisfactory approximation. Neglect of the scaled-MM interaction terms, as in Ref. [15], increases the energy of the products by about 6 kcal/mol.

Finally, we compare the results obtained with Mulliken charges to represent the QM atoms with those obtained with ESP charges [19, 20] (Fig. 5). Since the structures are the same, the step 1 energies, which are based on the exact QM/MM energies, are unchanged. The curves for steps II and III differ slightly but are similar overall because the charges obtained with the two methods are highly correlated (Pearson linear correlation coefficients greater than 0.9). This is not to say that the two sets of charges are the same; in general the ESP charges are larger in magnitude (root-mean-square value of about 0.5*e* compared with a root-mean-square value of about 0.3*e* for the Mulliken charges). However, the differences in steps II and III cancel for the most part so that the maximum deviation between the total energy curves is 1.8 kcal/mol. In principle other schemes (e.g., CM2 [34]) could be used to assign charges to the QM atoms. However, the similarities between the results obtained with Mulliken and ESP charges (only the latter of which reproduces the dipole moment of the system, as described in the legend to Fig. 5) suggest that the method is robust to reasonable variations in this aspect of the procedure.

5 Discussion

In the present paper, we have described an efficient method for treating the effects of solvent in QM/MM calculations. The method avoids the need for explicit solvent molecules, as in a periodic boundary simulation. Most solvent shielding is treated implicitly, but a limited number of explicit solvent molecules are included to

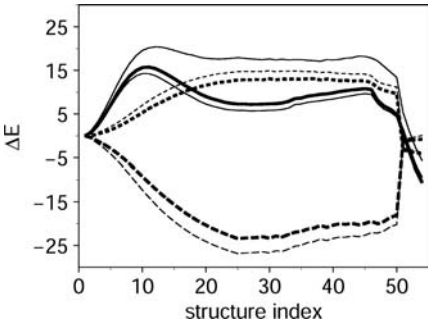

Fig. 5. Reaction profile obtained with electrostatic screening potential (*ESP*) charges representing the QM atoms. The ESP curves are *bold*, and the Mulliken curves shown for comparison are *thin*. The ESP charges were obtained by fitting the electrostatic potential calculated at the MM positions with the constraint that the sum of the atomic charges should reproduce the total charge and the components of the dipole of the quantum system. The root-mean-square error in the dipole moment was 3% of the magnitude of the exact dipole on average

allow the formation of directional hydrogen bonds to water molecules that are in or near the active site. In the procedure, which was originally introduced for MM free-energy-perturbation simulations [15], the charges of exposed ionizable groups are scaled for the QM/MM calculation (step I), and continuum electrostatics methods are used to quantitatively correct the energies (steps II and III). The primary modifications made to the scheme outlined in Ref. [15] are the use of Mulliken or ESP charges to represent the QM atoms in the grid-based calculations and the inclusion of additional terms in step II to account for variations in the MM–MM interactions. The latter makes a difference in energy of about 6 kcal/mol for the products. Overall, the method yielded good agreement with experiment for the reaction catalyzed by UDG and made it possible to obtain a detailed understanding of the enzyme mechanism [16].

The procedure introduced for free-energy-perturbation simulations [15] builds on earlier work [35, 36, 37, 38]. Of particular interest for the present study is Ref. [35], in which enzyme charges were scaled according to a potential-based scheme to calculate the reaction profile for prolyl isomerization by FK506 binding protein. That study employed step I of the procedure to determine a reaction mechanism but did not correct for scaling the charges to obtain quantitatively correct energies. Since large charge shifts are not involved in that system, the correction is expected to be less important.

While a number of dielectric screening models have been introduced for purely QM calculations [39, 40, 41, 42, 43], they have not been used in QM/MM simulations. One problem with such treatments, as pointed out in Ref. [44], is that hydrogen bonding is not treated well. Although the present treatment does not allow charge transfer between the QM region and the MM solvent, it does allow for the formation of directional hydrogen bonds, which have been shown to be important in QM/MM simulations of enzyme reactions [14].

An alternative to continuum dielectric methods is to represent the solvent and part of the protein by polarizable dipoles restricted to a grid (the Langevin dipoles and protein dipoles Langevin dipoles methods) [2, 45]. This method has been employed extensively in conjunction with empirical valence bond treatments of the reactive region [2] (for a recent example, see Ref. [46]). In a certain sense, the grid-based dipole model is a discrete version of the continuum methods, though there are differences in detail. The use of dipoles for the parts of the system treated implicitly obviates the need to select a dielectric constant but requires analogous parameterization (i.e., the polarizability of the dipoles). While the solvent dielectric response can be anisotropic, the dipole model still does not fully capture the physics of explicit solvent molecules. Our results suggest that including a limited number of explicit solvent molecules in such calculations could be of interest.

The charge-scaling procedure described here represents a significant advance in the ability to treat solvent in QM/MM simulations. The present study employed a semiempirical Hamiltonian in the QM region, but the procedure is not limited to any particular QM or MM method. In fact, its use is likely to be more important for ab initio and density functional theory Hamiltonians as well as polarizable MM force fields because these will all be more sensitive to long-range electrostatic interactions, so that good modeling of solvent shielding effects is essential. The increasing use of the methods just mentioned and the results obtained in the present work and Langevin dipole studies [2, 46] suggests that additional investigations as well as applications (e.g., molecular dynamics free energy simulations), of implicit solvent models for QM/MM simulations can be expected in the near future.

References

1. Field MJ, Bash PA, Karplus M (1990) J Comput Chem 11: 700–733
2. Warshel A (1991) Computer Modeling of Chemical Reactions in Enzymes and Solutions. Wiley New York
3. Kollman PA (1992) Curr Opin Struct Biol 2: 765–771
4. Eurenius KP, Chatfield DC, Brooks BR (1996) Int J Quantum Chem 60: 1189–1200
5. Cunningham MA, Bash PA (1997) Biochimie 79: 687–689
6. Friesner RA, Beachy MD (1998) Curr Opin Struct Biol 8: 257–262
7. Gogonea V, Suárez D, van der Vaart A, Merz KM Jr (2001) Curr Opin Struct Biol 11: 217–223
8. Jorgensen WI, Chandrasekhar J, Madura JD, Impey RW, Klein ML (1983) J Chem Phys 79: 926–935
9. Wesson L, Eisenberg D (1992) Protein Sci 1: 227–235
10. Lazaridis T, Karplus M (1999) Proteins 35: 133–152
11. Schaefer M, Karplus M (1996) J Phys Chem 100: 1578–1599
12. Neumann M (1985) J Chem Phys 82: 5663–5672
13. Kurtović Z, Marchi M, Chandler D (1993) Mol Phys 78: 1155–1165
14. Peräkylä M, Kollman PA (1997) J Am Chem Soc 119: 1189–1196
15. Simonson T, Archontis G, Karplus M (1997) J Phys Chem B 101: 8349–8362
16. Dinner AR, Blackburn GM, Karplus M (2001) Nature 413: 752–755
17. Santos JSO, Fischer S, Guilbert C, Lewit-Bentley A, Smith JC (2000) Biochemistry 39: 14065–14074
18. Brooks BR, Bruccoleri RE, Olafson BD, States DJ, Swaminathan S, Karplus M, (1983) J Comput Chem 4: 187–217
19. Singh UC, Kollman PA (1984) J Comput Chem 5: 129–145
20. Besler BH, Merz KM Jr, Kollman PA (1990) J Comput Chem 11: 431–439
21. Parikh SS, Walcher G, Jones GD, Slupphaug G, Krokan HE, Blackburn GM, Tainer JA (2000) Proc Natl Acad Sci USA 97: 5083–5088
22. Slupphaug G, Eftedal I, Kavli B, Bharati S, Helle NM, Haug T, Levine DW, Krokan HE (1995) Biochemistry 34: 128–138
23. Drohat AC, Xiao G, Tordova M, Jagadeesh J, Pankiewicz KW, Watanabe KA, Gilliland GL, Stivers JT (1999) Biochemistry 38: 11876–11886
24. Schaefer M, Sommer M, Karplus M (1997) J Phys Chem B 101: 1663–1683
25. Dewar MJS, Zoebisch EG, Healy EF Stewart JJP (1985) J Am Chem Soc 107: 3902–3909
26. MacKerell AD Jr, Wiórkiewicz-Kuczera J, Karplus M (1995) J Am Chem Soc 117: 11946–11975
27. MacKerell AD Jr, Bashford D, Bellott M, Dunbrack RL, Evanseck JD, Field MJ, Fischer S, Gao J, Guo H, Ha S, Joseph-McCarthy D, Kuchnir L, Kuczera K, Lau FTK, Mattos C, Michnick S, Ngo T, Nguyen DT, Prodhom B, Reiher WE, Roux B, Schlenkrich M, Smith JC, Stote R, Straub J, Watanabe M, Wiórkiewicz-Kuczera J, Yin D, Karplus M (1998) J Phys Chem B 102: 3586–3616

28. Neria E, Fischer S, Karplus M (1996) J Chem Phys 105: 1902–1921
29. Steinbach PJ, Brooks BR (1994) J Comput Chem 15: 667–683
30. Reuter N, Dejaegere A, Maigret B, Karplus M (2000) J Phys Chem A 104: 1720–1735
31. Werner RM, Stivers JT (2000) Biochemistry 39: 14054–14064
32. Vocadlo DJ, Davies GJ, Laine R, Withers SG (2001) Nature 412: 835–838
33. Bashford D, Karplus M (1990) Biochemistry 29: 10219–10225
34. Li J, Zhu T, Cramer CJ, Truhlar DG (1998) J Phys Chem A 102: 1820–1831
35. Fischer S, Michnick S, Karplus M (1993) Biochemistry 32: 13830–13837
36. Resat H, McCammon JA (1996) J Chem Phys 104: 7645–7651
37. Resat H, McCammon JA (1998) J Chem Phys 108: 9617–9623
38. Prévost M (1996) J Mol Biol 260: 99–110
39. Klamt A, Schuurmann G (1993) J Chem Soc Perkin Trans 2: 799–805
40. Tomasi J, Persico M (1994) Chem Rev 94: 2027–2094
41. Cortis CM, Langlois J-M, Beachy MD, Friesner RA (1996) J Chem Phys 105: 5472–5484
42. Barone V, Cossi M (1998) J Phys Chem A 102: 1995–2001
43. York DM, Karplus M (1999) J Phys Chem A 103: 11060–11079
44. Marten B, Kim K, Cortis C, Friesner RA, Murphy RB Ringnalda MN, Sitkoff D, Honig B (1996) J Phys Chem 100: 11775–11788
45. Warshel A, Russell ST (1984) Q Rev Biophys 17: 283–422
46. Várnai P, Warshel A (2000) J Am Chem Soc 122: 3849–3860